

# Analysis of Light Propagation in Optical Fibers with a High Step Index

P.S. JUNG\* AND M.A. KARPIERZ

Faculty of Physics, Warsaw University of Technology, Koszykowa 75, 00-662 Warsaw, Poland

Simulation of light beam propagation in optical fiber with a high step index requires the use of complicated methods. One of the simplest and accurate method is presented in this paper. The possibility of use of beam propagation method with exact boundary conditions in light beam propagation in optical fibers is shown in this work. The comparison of this method with analytical solutions for planar waveguide and optical fiber confirms usefulness of it.

PACS: 42.25.Bs, 42.81.-i, 42.81.Qb

## 1. Introduction

One of the basic method for analysis of the light beam propagation is beam propagation method (BPM) [1]. It has a lot of varieties such as finite differences (FD-BPM) [2, 3], finite elements (FE-BPM) [4, 5] or based on the fast Fourier transformation (FFT-BPM) [6]. These methods have the same disadvantages: they could be only used in a homogeneous region and an inhomogeneous one with a small step of the refractive index. Of course, there are known some approximations of the step index profile such as the graded index [7], the staircase index [8] or the average index [2]. Unfortunately, in most cases in structures such as microstructural fibers [9, 10], slot waveguides [11, 12], buried waveguides [13], photonic nanowires [14, 15] these approximations are not accurate enough [16], especially when a polarization is considered. The reason of it is that in above mentioned structures high step of the refractive index is observed, for instance between air and silica glass or air and silicon. This difference between refractive indices determines the electromagnetic field distributions during propagation and consequently has an influence on the polarization.

In Fig. 1 there are presented the guided modes in a planar waveguide for different polarizations and different value of step of the refractive indices. As it is seen for the case when the field is perpendicular to the surface, there is observed a step of the amplitude at the border according with increased electric permittivity. One of the ways to solve the problem of the high step of the refractive index for the FD-BPM in the scalar case was presented by Vassallo [17]. A more general method for structures with arbitrary shapes was presented by Chang et al. [18, 19]. However, a practical implementation of this method is complicated.

In this paper it is presented simpler (than that proposed by Chang) possibility of use FD-BPM together with exact boundary conditions (EBC) from the Maxwell equations to the analysis light beam propagation in optical fibers and waveguides with a high step index.

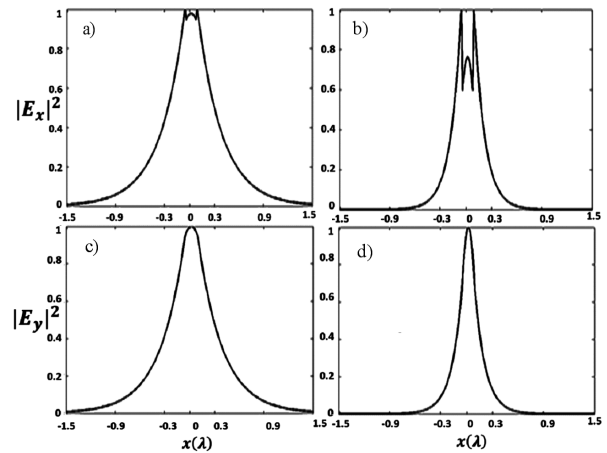


Fig. 1. The guided mode in a planar waveguide: for the TM polarization and the electric field perpendicular to the border: (a)  $\epsilon_{\text{core}} = 1.1025$ ,  $\epsilon_{\text{clad}} = 1$ , (b)  $\epsilon_{\text{core}} = 2.1025$ ,  $\epsilon_{\text{clad}} = 1$  and for the TE polarization and the electric field parallel to the border (c)  $\epsilon_{\text{core}} = 1.1025$ ,  $\epsilon_{\text{clad}} = 1$ , (d)  $\epsilon_{\text{core}} = 2.1025$ ,  $\epsilon_{\text{clad}} = 1$ .

## 2. Description of the method

In most cases BPM bases on the paraxial equation for the electric field

$$-2i\beta \frac{\partial}{\partial z} \mathbf{E} + \frac{\partial^2}{\partial x^2} \mathbf{E} + \frac{\partial^2}{\partial y^2} \mathbf{E} + \gamma(x, y)^2 \mathbf{E} = \mathbf{0}, \quad (1)$$

where  $\beta$  is a constant,  $\mathbf{E}$  is an amplitude of the electric field

\* corresponding author; e-mail: jung@if.pw.edu.pl

$$\mathbf{E}(x, y, z, t) = \mathbf{E}(x, y, z) e^{i\omega t - i\beta z}, \quad (2)$$

and  $\gamma$  is equal to

$$\gamma^2 = \frac{\omega^2}{c^2} \varepsilon - \beta^2, \quad (3)$$

$\varepsilon$  is electrical permittivity in medium. Using the coordinates in a discrete form as

$$\begin{cases} x = \Delta x N + x_0, \\ y = \Delta y M + y_0, \\ M, N = 1, 2, 3, \dots \end{cases} \quad (4)$$

Eq. (1) can be solved numerically, where in the simplest split-step BPM a discrete formula is written as

$$\begin{aligned} & \frac{E(N, M, z + \Delta z) - E(N, M, z)}{\Delta z} \\ &= \frac{1}{2i\beta} \left( \frac{E(N-1, M) + E(N+1, M) - 2E(N, M)}{\Delta x^2} \right. \\ &+ \frac{E(N, M-1) + E(N, M+1) - 2E(N, M)}{\Delta y^2} \\ &+ \left. \gamma(N, M)^2 E(N, M) \right). \end{aligned} \quad (5)$$

Amplitudes used at the right side of Eq. (5) are calculated in  $z$  or/and  $z + \Delta z$  depending on a method [20]. Changes of the refractive index are included only in changes of  $\gamma$  value.

Equation (1) is useful in a homogeneous medium ( $\nabla\varepsilon = 0$ ) and in an inhomogeneous one characterized by slowly varying of electric permittivity ( $\nabla\varepsilon/\varepsilon \ll 1/\lambda$ , where  $\lambda$  is the wavelength). This is a serious disadvantage of a useful paraxial equation, especially when it is considered a structure with a high step of the refractive index (as it is seen in Fig. 1), where the field perpendicular to the surface is discontinuous. Therefore, we propose an algorithm, where a propagation in homogeneous regions is calculated from Eqs. (1) and they are matched by proper EBC. The boundary conditions between two different media to consider polarization effects are obtained from the Maxwell equations [19]:

$$\varepsilon_1 \mathbf{E}_n^{(1)} = \varepsilon_2 \mathbf{E}_n^{(2)}, \quad (6)$$

$$\mathbf{E}_t^{(1)} = \mathbf{E}_t^{(2)}, \quad (7)$$

$$\frac{\partial}{\partial n} \mathbf{E}_n^{(1)} = \frac{\partial}{\partial n} \mathbf{E}_n^{(2)}, \quad (8)$$

$$\frac{\partial}{\partial n} \mathbf{E}_t^{(1)} = \frac{\partial}{\partial n} \mathbf{E}_t^{(2)} + \left( \frac{\varepsilon_2}{\varepsilon_1} - 1 \right) \frac{\partial}{\partial t} \mathbf{E}_n^{(2)}, \quad (9)$$

where indices t and n represent components which are parallel and perpendicular to the surface.

This EBC can be used for any algorithm, but in this paper we use algorithm based on the paraxial Eq. (1). Two components of an electric field in the same time (for curve structure is necessary) are used for calculations. The general established procedure of this algorithm is that the fields are calculated separately in homogeneous media i.e. in a medium with an electric permittivity  $\varepsilon_1$  there is field with an amplitude  $E^{(1)}$  and in a medium with an electric permittivity  $\varepsilon_2$  there is field with an am-

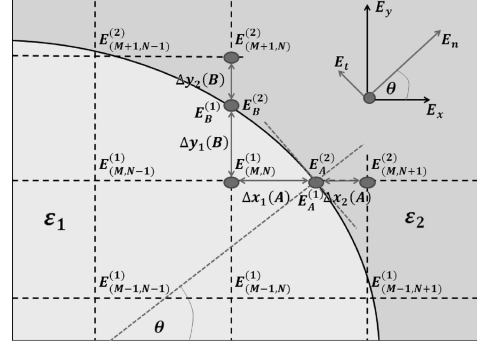


Fig. 2. Cross-section of the problem under border for optical fiber. The values  $E$  represent the electric field components  $E_x$ ,  $E_y$ ,  $E_t$ ,  $E_n$ .

plitude  $E^{(2)}$ . Solutions in neighboring media are matched at each step on the border by using boundary conditions (6)–(9). To receive an exact solution the border between two media must be stored (the distance between border and the nearest grid points in appropriate directions).

Because of the fact that considered structure is curved, as seen in Fig. 2, we make a local transformation of the field from Cartesian coordinates to cylindrical, as follows:

$$\begin{cases} E_n = E_x \cos \theta + E_y \sin \theta, \\ E_t = -E_x \sin \theta + E_y \cos \theta. \end{cases} \quad (10)$$

The boundary conditions (6)–(9) for the field at the border must be fulfilled for each point, where the lines cross the border line, like point  $A$  and  $B$  in Fig. 2. The point  $A$  lies in the  $\Delta y M + y_0 = \text{const}$  line (in the distance  $\Delta x_1(A)$  from line  $\Delta y M + y_0 = \text{const}$  and  $\Delta x_2(A)$  from line  $\Delta y(M+1) + y_0 = \text{const}$ ). Analogously, the point  $B$  lies in the  $\Delta x M + x_0 = \text{const}$  line. Using this notation, Eqs. (6), (7) can be rewritten in a discrete form

$$\varepsilon_1 E_n^{(1)}(A) = \varepsilon_2 E_n^{(2)}(A), \quad (11)$$

$$\varepsilon_1 E_n^{(1)}(B) = \varepsilon_2 E_n^{(2)}(B), \quad (12)$$

$$E_t^{(1)}(A) = E_t^{(2)}(A), \quad (13)$$

$$E_t^{(1)}(B) = E_t^{(2)}(B) \quad (14)$$

and from Eqs. (8), (9) we propose an approximation

$$\begin{aligned} & \frac{E_n^{(1)}(A) - E_n^{(1)}(M, N)}{\Delta x_1} \\ &= \frac{E_n^{(2)}(M, N+1) - E_n^{(2)}(A)}{\Delta x_2}, \end{aligned} \quad (15)$$

$$\begin{aligned} & \frac{E_n^{(1)}(B) - E_n^{(1)}(M, N)}{\Delta y_1} \\ &= \frac{E_n^{(2)}(M+1, N) - E_n^{(2)}(B)}{\Delta y_2}, \end{aligned} \quad (16)$$

$$\begin{aligned} & \frac{E_t^{(1)}(A) - E_t^{(1)}(M, N)}{\Delta x_1} \\ &= \frac{E_t^{(2)}(M, N+1) - E_t^{(2)}(A)}{\Delta x_2}, \end{aligned} \quad (17)$$

$$\begin{aligned} & \frac{E_t^{(1)}(B) - E_t^{(1)}(M, N)}{\Delta y_1} \\ &= \frac{E_t^{(2)}(M+1, N) - E_t^{(2)}(B)}{\Delta y_2}. \end{aligned} \quad (18)$$

If we assume that

$$\begin{aligned} & \frac{E_n^{(1)}(A) - E_n^{(1)}(M, N)}{\Delta x_1} \\ & \approx \frac{E_n^{(1)}(M, N+1) - E_n^{(1)}(M, N)}{\Delta x} \end{aligned} \quad (19)$$

and analogous relations for other derivatives for neighboring points, the following relations from (11)–(18) are obtained:

$$\begin{aligned} E_n^{(1)}(M, N+1) &= \left(1 - \frac{\Delta x}{\Delta x_1}\right) E_n^{(1)}(M, N) + \frac{\Delta x}{\Delta x_1} \\ & \times \frac{\Delta x_1 E_n^{(2)}(M, N+1) + \Delta x_2 E_n^{(1)}(M, N)}{\Delta x_2 + \Delta x_1 \frac{\varepsilon_1}{\varepsilon_2}}, \end{aligned} \quad (20)$$

$$\begin{aligned} E_n^{(1)}(M+1, N) &= \left(1 - \frac{\Delta y}{\Delta y_1}\right) E_n^{(1)}(M, N) + \frac{\Delta y}{\Delta y_1} \\ & \times \frac{\Delta y_1 E_n^{(2)}(M, N+1) + \Delta y_2 E_n^{(1)}(M, N)}{\Delta y_2 + \Delta y_1 \frac{\varepsilon_1}{\varepsilon_2}}, \end{aligned} \quad (21)$$

$$\begin{aligned} E_t^{(1)}(M, N+1) &= \left(1 - \frac{\Delta x}{\Delta x_1}\right) E_t^{(1)}(M, N) + \frac{\Delta x}{\Delta x_1} \\ & \times \frac{\Delta x_1 E_t^{(2)}(M+1, N) + \Delta x_2 E_t^{(1)}(M, N)}{\Delta x_2 + \Delta x_1}, \end{aligned} \quad (22)$$

$$\begin{aligned} E_t^{(1)}(M+1, N) &= \left(1 - \frac{\Delta y}{\Delta y_1}\right) E_t^{(1)}(M, N) + \frac{\Delta y}{\Delta y_1} \\ & \times \frac{\Delta y_1 E_t^{(2)}(M+1, N) + \Delta y_2 E_t^{(1)}(M, N)}{\Delta y_2 + \Delta y_1}. \end{aligned} \quad (23)$$

The fields  $E_n^{(2)}(MN)$  and  $E_t^{(2)}(MN)$  can be calculated analogously.

The last step is to do the inverse transformation, and back to Cartesian coordinates system by the following relations:

$$\begin{cases} E_x = E_r \cos \theta - E_\theta \sin \theta, \\ E_y = E_r \sin \theta + E_\theta \cos \theta. \end{cases} \quad (24)$$

Summarizing, in order to use Eq. (5) to calculate the field in the next plane at point  $E^{(1)}(y, x)$  near the border for the medium “1”, we should know the value at point  $E^{(1)}(y, x + \Delta x)$  or  $E^{(1)}(y, x - \Delta x)$  and  $E^{(1)}(y + \Delta y, x)$  or  $E^{(1)}(y - \Delta y, x)$  outside the border and in medium ‘2’ to calculate the field  $E^{(2)}(y, x)$  the value at point  $E^{(2)}(y, x + \Delta x)$  or  $E^{(2)}(y, x - \Delta x)$  and  $E^{(2)}(y + \Delta y, x)$  or  $E^{(2)}(y - \Delta y, x)$  must be known. In this case the conditions from Eqs. (11)–(22) are used.

### 3. Numerical results

The first presented results showed a (1+1) dimension beam propagating in the planar waveguide (Fig. 3a). The material parameters used in simulations correspond to

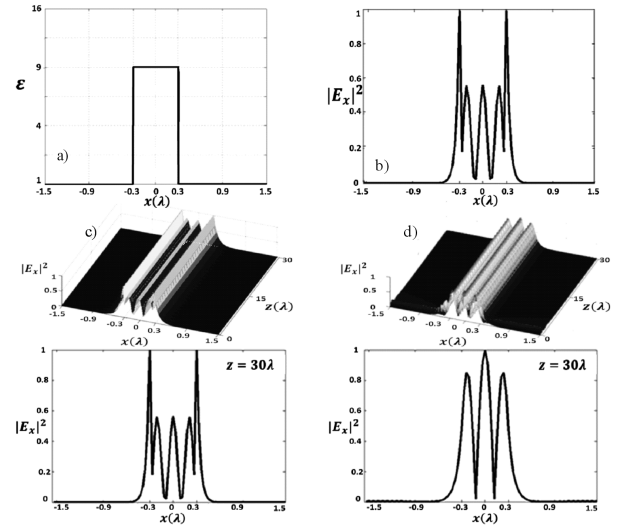


Fig. 3. Simulations for: (a) the planar waveguide with (b) the guided mode calculated analytically, (c) beam propagation for the BPM with EBC, and (d) classical BPM.

the electric permittivity of the cladding  $\varepsilon_{\text{clad}} = 1$ , electric permittivity of the core  $\varepsilon_{\text{core}} = 9$  and the width of the core is  $0.6\lambda$ . The guided mode for an examined structure is seen in Fig. 3b. Simulations were done for a proposed method and classical BPM based only on paraxial Eqs. (1). In both cases simulations were run for a launched beam corresponding an analytical solution of the guided mode.

Light is guided in the area of a higher refractive index in both case. But in the conventional BPM discontinuities of the field distribution at borders between the core and the cladding are disappearing at a very short distance of propagation (Fig. 3d). The situation is quite different in simulations using the BPM with EBC (Fig. 3c). Moreover, the field distribution after  $30\lambda$  is the same as analytical solutions.

The simulation presented in Fig. 4 was done for (2+1) dimension beam propagation in cylindrical fibers. The first (Fig. 4a) has the electric permittivity of the cladding  $\varepsilon_{\text{clad}} = 1$ , the electric permittivity of the core  $\varepsilon_{\text{core}} = 1.96$  and the radius of the core is  $0.4\lambda$ . The second fiber differs only with the electric permittivity of the core  $\varepsilon_{\text{core}} = 5.76$  and the radius of the core is  $0.2\lambda$ . The guided mode for examined structures are seen in Fig. 4c,d. The different value of the refractive index core causes a higher step of the amplitude at the border in  $x$  direction. The simulations were done similarly, as it was for the planar waveguide. Two methods, BPM and BPM with EBC were used. Also, in both cases, simulations were run for a launched beam corresponding to an analytical solution of the guided mode.

The results of the propagation at a distance  $30\lambda$  are shown in Fig. 4e,f (for conventional BPM) and in Fig. 4g,h (for proposed method). In the conventional BPM discontinuities of the field distribution at borders

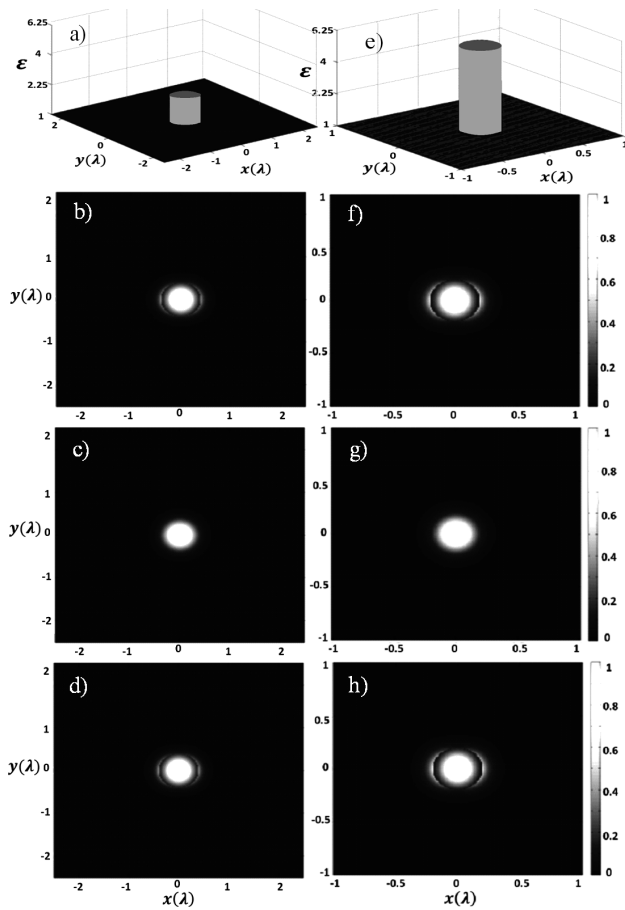


Fig. 4. Simulations for: (a) an optical fiber with (c) the guided mode of the  $x$  component of the electric field, (e) distribution of the field received after distance  $30\lambda$  for classical BPM and (g) for BPM with EBC. Analogously, parts (d, f, h) are for an optical fiber (b).

between the core and the cladding disappear for both fibers (Fig. 4e,f). The received distributions for the  $x$  component electric field from simulations for BPM with EBC (Fig. 4g,h) are the same as guided modes. In both cases it is observed a discontinuity of the field in  $x$  direction.

In all numerical calculations the Runge–Kutta (RK4) [21] algorithm was used to speed up simulations and perfect matched layers (PML) [20] to reduce reflections from a computational window.

#### 4. Conclusions

Summarizing, we proposed the implementation of the BPM with relatively simple form of EBC. The proposed

method can be used for analysis of beam propagation in dielectric structures with high step of a refractive index. This was confirmed by showing results in (1+1)D case in the planar waveguide and in (2+1)D case in optical fibers.

#### References

- [1] J.E. Midwinter, *Optical Fibers for Transmission*, Wiley, New York 1979.
- [2] Z. Zhu, T.G. Brown, *Opt. Expr.* **10**, 853 (2002).
- [3] M. Kwaśny, U.A. Laudyn, P. Jung, M.A. Karpierz, *Photon. Lett. Poland* **1**, 160 (2009).
- [4] Y. Tsuji, M. Koshiba, *Int. J. Numer. Model* **13**, 115 (2000).
- [5] M. Eguchi, *J. Opt. Soc. Am. B* **27**, 1464 (2010).
- [6] J.M. López-Doña, J.G. Wangüemert-Pérez, I. Molina-Fernández, *IEEE Photon. Technol. Lett.* **17**, 387 (2005).
- [7] G.R. Hadley, *IEEE J. Quantum Electron.* **28**, 363 (1992).
- [8] K. Bierwirth, N. Schulz, F. Arndt, *IEEE Trans. Microw. Theory Technol.* **34**, 1104 (1986).
- [9] J.M. Fini, *Meas. Sci. Technol.* **15**, 1120 (2004).
- [10] C.M.D. Cordeiro, M.A.R. Franco, G. Chesini, E.C.S. Barretto, R. Lwin, C.H.B. Cruz, M. Large, *Opt. Expr.* **14**, 13056 (2006).
- [11] C.A. Barrios, K.B. Gylfason, B. Sánchez, A. Griol, H. Sohlström, M. Holgado, R. Casquel, *Opt. Lett.* **32**, 3080 (2007).
- [12] C.A. Barrios, B. Sánchez, K.B. Gylfason, A. Griol, H. Sohlström, M. Holgado, R. Casquel, *Opt. Expr.* **15**, 6846 (2007).
- [13] J. Grelin, E. Ghibaudo, J.E. Broquin, *Mater. Sci. Eng. B* **149**, 185 (2008).
- [14] R. Yan, D. Gargas, P. Yang, *Nat. Photonics* **3**, 569 (2009).
- [15] H. Lu, X. Liu, Y. Gong, X. Hu, X. Li, *J. Opt. Soc. Am. B.* **27**, 904 (2010).
- [16] K.B. Zegadło, M.A. Karpierz, *Opto-Electron. Rev.* **20**, 42 (2012).
- [17] C. Vassallo, *Proc. Inst. Elect. Eng. J* **139**, 137 (1992).
- [18] Y.-C. Chiang, Y.-P. Chiou, H.-C. Chang, *J. Lightwave Technol.* **20**, 2371 (2002).
- [19] Y.-C. Chiang, Y.-P. Chiou, H.-C. Chang, *J. Lightwave Technol.* **26**, 3107 (2008).
- [20] J.P. Berenger, *J. Comput. Phys.* **114**, 185 (1994).
- [21] H.W. Press, S.A. Teukolsky, W.T. Vetterling, B.P. Flannery, *The Art of Scientific Computing*, 2nd ed., Cambridge University Press, New York 1992.